

# Effects of the Symmetry Energy and its Slope on Neutron Star Properties

Luiz L. Lopes<sup>1,2,\*</sup> and Debora P. Menezes<sup>1</sup>

<sup>1</sup>*Departamento de Física, CFM - Universidade Federal de Santa Catarina; C.P. 476, CEP 88.040-900, Florianópolis, SC, Brasil*

<sup>2</sup>*Centro Federal de Educação Tecnológica de Minas Gerais Campus VIII; CEP 37.022-56, Varginha - MG - Brasil*

(Dated: October 3, 2018)

In this work we study the influence of the symmetry energy and its slope on three major properties of neutron stars: the maximum mass, the radii of the canonical  $1.4M_{\odot}$  and the minimum mass that enables the direct URCA effect. We utilize four parametrizations of the relativistic quantum hydrodynamics and vary the symmetry energy within accepted values. We see that although the maximum mass is almost independent of it, the radius of the canonical  $1.4M_{\odot}$  and the mass that enables the direct URCA effect is strongly correlated with the symmetry energy and its slope. Also, since we expect that the radius grows with the slope, a theoretical limit arises when we increase this quantity above certain values.

PACS numbers: 21.65.Ef, 24.10.Jv, 26.60.Kp

## I. INTRODUCTION

Although nuclear matter properties are well known around the saturation point, the physics of very high density and strongly isospin-asymmetric matter is far from being completely understood. This extreme region is important to determine the main properties of an exotic object, the neutron star. Neutron stars are compact objects maintained by the equilibrium of gravity and the degenerescence pressure of the fermions together with a strong nuclear repulsion force due to the high density reached in their interior.

In the present work we focus on the properties of nuclear matter at sub-threshold density, which we describe with the relativistic quantum hydrodynamics (QHD) [1]. QHD is an effective model where the strong interaction is simulated by the exchange of massive mesons through Yukawa potentials. In the present work, we use the scalar-isoscalar  $\sigma$  meson, and the vector-isoscalar  $\omega$  meson to describe the properties of symmetric nuclear matter, and the vector-isovector  $\rho$  meson to correct the value of the symmetry energy [2] and describe effects of isospin-asymmetric matter. This  $\sigma\omega\rho$  model is the standard model of QHD in the current literature [3–5]. Within this model, once the coupling constant of the  $\rho$  meson is fixed the symmetry energy and its slope are established. Since the slope of the symmetry energy is important to constrain the neutron stars radii [6], another parameter is necessary if one wants to vary the slope without varying the symmetry energy and vice-versa. To accomplish this task, we include the scalar-isovector  $\delta$  [ $a_0(980)$ ] meson in a more complete  $\sigma\omega\rho\delta$  model [7, 8]. The effects of the  $\delta$  meson in asymmetric matter were already studied in several topics as the neutron radii [9], linear response [7, 8, 10] and even neutron star properties [11, 12], however, in a different approach. Instead of worrying about the strength of the coupling constant

of the delta meson with the baryons [8, 11, 12], what is strongly model dependent, we focus on the fitting of the physical quantities given by the symmetry energy and its slope.

There are many different parametrizations for the QHD models in the literature, all of them chosen so as to reproduce nuclear matter bulk properties. In a recent work [13], an extensive review of 263 parametrizations of different types of RMF models were analysed under three different sets of constraints related to symmetric nuclear matter, pure neutron matter, symmetry energy, and its derivatives. In this paper, we utilize four of these parametrizations: GM1, GM3 [14], NL $\rho$  [8] and NL3 [15] to describe the properties of symmetric nuclear matter. Not all of them satisfy the constraints investigated in [13], but we perform some modifications on the usual parameters based on the symmetry energy and its slope and in the conclusions section, we discuss possible constraints related to neutron star observational properties. The value of the symmetry energy at saturation density is well known to lie between 30 MeV and 35 MeV [16–18]. The value of the symmetry energy slope is rather more controversial. Although some results point towards a very low value of slope, lower than 62 MeV [19, 20], other studies indicate a much higher limit, up to 113 MeV [16, 21]. We follow this last prescription which is very close to the limit of 115 MeV presented in Ref. [13]. Nevertheless, we can find in the literature values as high as 150 MeV [11] or even higher than 170 MeV, as pointed out in a recent work [22].

We study the influence of the energy symmetry and its slope on three major properties of neutron stars: the maximum mass, the radius of the canonical  $1.4M_{\odot}$  and the minimum mass that enables direct URCA effect. To investigate these effects we utilize three different approaches. First, within the traditional  $\sigma\omega\rho$  models, we vary the symmetry between acceptable values. After, in order to investigate the individual effects of symmetry energy and the slope, we fix  $L$  and vary  $S_0$  within the  $\sigma\omega\rho\delta$  models. And then we perform the inverse situation, fixing  $S_0$  and varying  $L$ .

---

\* llopes@varginha.cefetmg.br

This paper is organized as follows: we review the formalism of the QHD models with and without the  $\delta$  meson and the parametrizations used in this work. Then we present the numerical results for the three approaches and discuss the implications and validity of the results.

Finally we present the conclusions of our work.

## II. THE FORMALISM

We use an extended version of the relativistic QHD [1], whose Lagrangian density reads:

$$\begin{aligned} \mathcal{L}_{QHD} = & \bar{\psi}_N [\gamma^\mu (i\partial_\mu - g_v\omega_\mu - g_\rho \frac{1}{2}\vec{\tau} \cdot \vec{\rho}_\mu) - (m_N - g_s\sigma - g_\delta\vec{\tau} \cdot \vec{\delta})] \psi_N + \frac{1}{2}(\partial_\mu\sigma\partial^\mu\sigma - m_s^2\sigma^2) \\ & + \frac{1}{2}(\partial_\mu\vec{\delta}\partial^\mu\vec{\delta} - m_\delta^2\delta^2) - U(\sigma) + \frac{1}{2}m_v^2\omega_\mu\omega^\mu + \frac{1}{2}m_\rho^2\vec{\rho}_\mu \cdot \vec{\rho}^\mu - \frac{1}{4}\Omega^{\mu\nu}\Omega_{\mu\nu} - \frac{1}{4}\mathbf{P}^{\mu\nu} \cdot \mathbf{P}_{\mu\nu}, \end{aligned} \quad (1)$$

where  $\psi_N$  are the baryonic Dirac fields of the nucleons, and  $\sigma$ ,  $\omega_\mu$ ,  $\vec{\delta}$  and  $\vec{\rho}_\mu$  are the mesonic fields. The  $g$ 's are the Yukawa coupling constants that simulate the strong interaction,  $m_N$  is the mass of the nucleon (that we assume next as 939 MeV),  $m_s$ ,  $m_v$ ,  $m_\delta$  and  $m_\rho$  are the masses of the  $\sigma$ ,  $\omega$ ,  $\delta$  and  $\rho$  mesons respectively. The antisymmetric mesonic field strength tensors are given by their usual expressions as presented in [3]. The  $U(\sigma)$  is the self-interaction term introduced in ref. [23] to fix some of the saturation properties of the nuclear matter and is given by:

$$U(\sigma) = \frac{1}{3!}\kappa\sigma^3 + \frac{1}{4!}\lambda\sigma^4. \quad (2)$$

Finally,  $\vec{\tau}$  are the Pauli matrices. In order to describe a neutral, beta stable nuclear matter, we add leptons as free Fermi gases:

$$\mathcal{L}_{lep} = \sum_l \bar{\psi}_l [i\gamma^\mu\partial_\mu - m_l]\psi_l, \quad (3)$$

The electron and muon masses are 0.511 MeV and 105.6 MeV respectively.

To solve the equations of motion, we use the mean field approximation (MFA), where the meson fields are replaced by their expectation values, i.e:  $\sigma \rightarrow \langle\sigma\rangle = \sigma_0$ ,  $\delta \rightarrow \langle\delta\rangle = \delta_0$ ,  $\omega^\mu \rightarrow \delta_{0\mu}\langle\omega^\mu\rangle = \omega_0$  and  $\rho^\mu \rightarrow \delta_{0\mu}\langle\rho^\mu\rangle = \rho_0$ . The MFA gives us the following eigenvalue for the nucleon energy [3]:

$$E_N = \sqrt{k^2 + M_N^{*2}} + g_v\omega_0 + g_\rho\frac{\tau_3}{2}\rho_0, \quad (4)$$

where  $M_N^*$  is the nucleon effective mass:

$$M_N^* \doteq m_N - g_s\sigma_0 - g_\delta\tau_3\delta_0. \quad (5)$$

We see that while the vector-isovector  $\rho$  meson splits the energies, the scalar-isovector  $\delta$  meson splits the masses of the nucleons. The third Pauli matrix  $\tau_3$  assumes the value +1 (-1) for protons (neutrons).

For the leptons, the energy eigenvalues are those of the free Fermi gas:

$$E_l = \sqrt{k^2 + m_l^2}, \quad (6)$$

and the meson fields become:

$$\omega_0 = \frac{g_v}{m_s^2}(n_p + n_n), \quad (7)$$

$$\delta_0 = \frac{g_\delta}{m_\delta^2}(n_{Sp} - n_{Sn}), \quad (8)$$

$$\rho_0 = \frac{g_\rho}{m_\rho^2}\frac{1}{2}(n_p - n_n), \quad (9)$$

$$\sigma_0 = \frac{g_\sigma}{m_s^2}(n_{Sp} + n_{Sn}) - \frac{1}{2}\frac{\kappa}{m_s^2}\sigma_0^2 - \frac{1}{6}\frac{\lambda}{m_s^2}\sigma_0^3, \quad (10)$$

where  $n_{Sp}$ ,  $n_{Sn}$  are the scalar densities, and  $n_p$  and  $n_n$  are the number densities of the protons and the neutrons respectively and are given by:

$$\begin{aligned} n_{SB} &= \int_0^{k_{fB}} \frac{M_B^*}{\sqrt{k^2 + M_B^{*2}}} \frac{k^2}{\pi^2} dk, \\ n_B &= \frac{k_{fB}^3}{3\pi^2}, \quad \text{and} \quad n = \sum_B n_B, \\ B &= (p, n). \end{aligned} \quad (11)$$

To describe the properties of the nuclear matter, we calculate the EoS from statistical mechanics [24]. The nucleons and leptons, being fermions, obey the Fermi-Dirac distribution. In order to compare our results with experimental and observational constraints, we next study nuclear and stellar systems at zero temperature. In this case the Fermi-Dirac distribution becomes the Heaviside step function. The energy densities of baryons, leptons and mesons read:

$$\epsilon_B = \frac{1}{\pi^2} \sum_B \int_0^{k_f} \sqrt{k^2 + M_B^{*2}} k^2 dk, \quad (12)$$

$$\epsilon_l = \frac{1}{\pi^2} \sum_l \int_0^{k_f} \sqrt{k^2 + m_l^2} k^2 dk, \quad (13)$$

$$\epsilon_m = \frac{1}{2} \left( m_s^2 \sigma_0^2 + m_v^2 \omega_0^2 + m_\delta^2 \delta_0^2 + m_\rho^2 \rho_0^2 \right) + U(\sigma), \quad (14)$$

where  $k_f$  is the Fermi momentum, and we have already used the fact that the fermions have degeneracy equal to 2. The total energy density is the sum of the partial ones:

$$\epsilon = \epsilon_B + \epsilon_l + \epsilon_m, \quad (15)$$

and the pressure is calculated via thermodynamic relations:

$$P = \sum_f \mu_f n_f - \epsilon, \quad (16)$$

where the sum runs over all the fermions ( $f = B, l$ ) and  $\mu$  is the chemical potential, which corresponds exactly to the energy eigenvalue at  $T = 0$ .

Now we couple the equations imposing  $\beta$  equilibrium and zero total net charge:

$$\mu_p = \mu_n - \mu_e, \quad \mu_e = \mu_\mu, \quad n_p + \sum_l n_l = 0, \quad (17)$$

where  $\mu_p$ ,  $\mu_n$ ,  $\mu_e$  and  $\mu_\mu$  are the chemical potentials of the proton, neutron, electron and muon respectively.

The equation of states developed in this work are used as input to solve the Tolman-Oppenheimer-Volkoff (TOV) equations [25], that describe a static, spherically symmetric, relativistic star in hydrostatic equilibrium. The neutron star crust is simulated by the BPS EoS [26].

To compare the different approaches we need the symmetry energy of the symmetric nuclear matter ( $n_p = n_n$ ), which is defined as [6–8]:

$$S = \frac{1}{8} \left( \frac{g_\rho}{m_\rho} \right)^2 + \frac{k_f^2}{6\sqrt{k_f^2 + M^{*2}}} - \left( \frac{g_\delta}{m_\delta} \right)^2 \frac{M^{*2} n}{2(k_f^2 + M^{*2})[1 + (g_\delta/m_\delta)^2 \cdot A(k_f)]}, \quad (18)$$

where

$$A(k_f) = \frac{4}{(2\pi)^3} \int_0^{k_f} d^3k \frac{k^2}{k^2 + M^{*2}}, \quad (19)$$

is a function of the Fermi momentum ( $k_f = k_{fp} = k_{fn}$ ) and the effective mass ( $M^* = M_p^* = M_n^*$ ) of symmetric nuclear matter. According to Eq.(18), to fit the bulk properties of nuclear matter, we are not able to fix  $(g_\rho/m_\rho)^2$  and  $(g_\delta/m_\delta)^2$  independently. We then explore a family of values that allow the symmetry energy to lie between 30 and 35 MeV, bearing in mind that a maximum value  $(g_\delta/m_\delta)^2 = 2.6 \text{ fm}^{-2}$  arises from the so called *BonnC* potential [7, 8, 27].

It is useful to expand the symmetry energy  $S$  around the saturation density ( $n_0$ ) in a Taylor series as [16]:

$$S = S_0 + L\epsilon + O(\epsilon)^2, \quad (20)$$

where  $S_0$  is the symmetry energy at nuclear saturation point, and  $\epsilon = (n_0 - n)/3n_0$ . The parameter  $L$  is the so called slope of the symmetry energy, and is calculated at nuclear saturation density as:

$$L = 3n \left( \frac{dS}{dn} \right) \Big|_{n=n_0}. \quad (21)$$

We can also define the slope for an arbitrary density  $L(n)$  as [28]:

$$L(n) = 3n \left( \frac{dS}{dn} \right). \quad (22)$$

### III. MODEL PARAMETERS AND RESULTS

We utilize four well-known QHD parametrizations to fit the properties of nuclear saturation density. The nuclear saturation density,  $n_0$ ; binding energy per baryon,  $B/A$ , the effective nucleon mass,  $M^*$  and the nuclear compression modulus  $K$  are fixed parameters and are presented in Table I alongside the symmetry energy  $S_0$  and its slope  $L$ .

	GM1 [14]	GM3 [14]	NL3 [15]	NL $\rho$ [8]
$(g_s/m_s)^2 \text{ (fm}^{-2}\text{)}$	11.79	9.927	15.746	10.330
$(g_v/m_v)^2 \text{ (fm}^{-2}\text{)}$	7.149	4.820	10.516	5.421
$(g_\rho/m_\rho)^2 \text{ (fm}^{-2}\text{)}$	4.410	4.791	5.360	3.830
$\kappa/M_N$	0.005894	0.017318	0.0041014	0.01387
$\lambda$	-0.006426	-0.014526	-0.015921	-0.0288
$n_0 \text{ (fm}^{-3}\text{)}$	0.153	0.153	0.148	0.160
$M^*/M$	0.70	0.78	0.60	0.75
$K \text{ (MeV)}$	300	240	272	240
$B/A \text{ (MeV)}$	-16.3	-16.3	-16.3	-16.0
$S_0 \text{ (MeV)}$	32.49	32.49	37.40	30.49
$L \text{ (MeV)}$	93.7	89.7	118.4	85.0

TABLE I. Parameters and physical quantities for the original GM1, GM3, NL3 and NL $\rho$  models.

Nevertheless, we consider the symmetry energy and its slope as free parameter and divide this subject in three parts.

### A. No $\delta$ meson

We first study the influence of  $S_0$  and  $L$  without the  $\delta$  meson, where the  $\rho$  meson determines simultaneously the symmetry energy and its slope. The parameters utilized in this approach are presented in Tables II, III, IV and V for GM1, GM3, NL3 and NL $\rho$  respectively. It is worth noting that the original NL3 [15] has the values of 37.4 MeV and 118.4 MeV for  $S_0$  and  $L$  respectively. Both values are in disagreement with the experimental constraints [13, 16, 21]. However, we can fix this problem by redefining the coupling constant of the  $\rho$  meson, requiring that the symmetry energy assumes reasonable values.

From Tables II to V, we see that without  $\delta$  meson, the symmetry energy slope shows a perfect linear dependence with  $S_0$ . This effect is independent of the parametrization:

$$L = 3S_0 + C, \quad (23)$$

where the constant  $C$  is model dependent, but the angular coefficient is not.

$(g_\rho/m_\rho)^2 (fm^{-2})$	$(g_\delta/m_\delta)^2 (fm^{-2})$	$S_0$ (MeV)	$L$ (MeV)
3.880	-	30.49	87.9
4.145	-	31.49	90.9
4.410	-	32.49	93.9
4.677	-	33.49	96.9
4.936	-	34.49	99.9

TABLE II.  $S_0$  and  $L$  values for GM1 parametrization without  $\delta$  meson

$(g_\rho/m_\rho)^2 (fm^{-2})$	$(g_\delta/m_\delta)^2 (fm^{-2})$	$S_0$ (MeV)	$L$ (MeV)
4.260	-	30.49	83.7
4.525	-	31.49	86.7
4.791	-	32.49	89.7
5.055	-	33.49	92.7
5.319	-	34.49	95.7

TABLE III.  $S_0$  and  $L$  values for GM3 parametrization without  $\delta$  meson

$(g_\rho/m_\rho)^2 (fm^{-2})$	$(g_\delta/m_\delta)^2 (fm^{-2})$	$S_0$ (MeV)	$L$ (MeV)
3.458	-	30.40	97.4
3.733	-	31.40	100.4
4.006	-	32.40	103.4
4.280	-	33.40	106.4
4.552	-	34.40	109.4

TABLE IV.  $S_0$  and  $L$  values for NL3 parametrization without  $\delta$  meson

$(g_\rho/m_\rho)^2 (fm^{-2})$	$(g_\delta/m_\delta)^2 (fm^{-2})$	$S_0$ (MeV)	$L$ (MeV)
3.830	-	30.49	85.0
4.082	-	31.49	88.0
4.335	-	32.49	91.0
4.558	-	33.49	94.0
4.842	-	34.49	97.0

TABLE V.  $S_0$  and  $L$  values for NL $\rho$  parametrization without  $\delta$  meson

Without the  $\delta$  meson, the variation of the symmetry energy  $S_0$  implies a variation of the slope  $L$ . The symmetry energy  $S$  (Eq.(18)) and the slope for arbitrary densities  $L(n)$  (Eq.(22)) for GM1 and NL3 are plotted in Fig.1.

We see that the symmetry energy and the slope grows with the density and their lines never cross each other. In other words, the parametrization with lower symmetry energy and slope at low densities remains the parametrization with lower symmetry energy and slope at high densities. The behaviour of GM3 and NL $\rho$  are similar to those showed in Fig. 1.

Now, we solve the TOV equations [25] and plot the results in Fig.2. The symmetry energy and its slope have very little influence on the radii and almost zero influence on the maximum masses. Indeed, the radii of the  $1.4M_\odot$  varies about 0.2 km in all four parametrizations, always increasing with the symmetry energy and the slope, while the the maximum masses vary less than  $0.02M_\odot$ .

Lets us turn now to the direct URCA process. Cooling of the neutron star by neutrino emission can occur much faster if direct URCA process is allowed [29]. The direct URCA (DU) process takes place when the proton fraction exceeds a critical value  $x_{DU}$ , which can be evaluated in terms of the leptonic fraction [29, 30]:

$$x_{DU} = \frac{1}{1 + (1 + x_e^{1/3})^3}, \quad (24)$$

where  $x_e = n_e/(n_e + n_\mu)$ , and  $n_e$ ,  $n_\mu$  are the number densities of the electron and the muon respectively. We plot the proton fractions and the corresponding neutron star masses that allow DU process for the four parametrizations in Figs. 3 and 4 respectively. Although the macroscopic properties of the neutron stars suffer almost no influence from the symmetry energy and its slope, the minimum mass that enables DU process is strongly affected by them, and could vary up to 25 %, reaching  $0.3M_\odot$ .

The possibility of DU process in neutron star interiors is a subject of several studies [6, 30–34] and some ambiguities are still present. While non relativistic models predict a minimum mass of  $1.35M_\odot$  [30] or even higher [31] to allow the DU process to occur, relativistic models indicate that the minimum mass is as low as  $0.8M_\odot$  [32]. Although there is no consensus about the minimum mass that is able to trigger the DU process, it is reasonable to

assume  $1.1M_{\odot}$  as an inferior limit [33]. In this case, almost all the parametrizations without  $\delta$  meson should be avoided, as can be seen from by Fig. 4.

We resume the main results of this section in Table VI. In general, the parametrizations that predict higher maximum masses also predict larger radii for the canonical mass and higher minimum mass that enables DU process. However, this is not a general rule, since NL $\rho$  predicts a higher mass than GM3 ( $2.11 M_{\odot}$  vs  $2.04 M_{\odot}$ ) even with a lower radius value for the  $1.4M_{\odot}$  ( $12.93$  km vs  $13.07$  km). Also, one can notice that the NL $\rho$  has a bigger slope than GM3 ( $85.0$  MeV vs  $83.7$  MeV with the  $S_0 = 30.49$ ), indicating that the knowledge of the slope  $L$  is not enough to infer the neutron star radius.

Model	$S_0$ (MeV)	$M_{max}/M_{\odot}$	$R_{1.4M_{\odot}}$	$M_{DU}/M_{\odot}$	$n_{DU} (fm^{-3})$
GM1	30.49	2.39	13.72	1.26	0.305
GM1	31.49	2.39	13.76	1.17	0.290
GM1	32.49	2.39	13.80	1.10	0.279
GM1	33.49	2.38	13.84	1.04	0.267
GM1	34.49	2.38	13.91	0.98	0.255
GM3	30.49	2.04	13.07	1.10	0.327
GM3	31.49	2.04	13.12	1.04	0.309
GM3	32.49	2.04	13.16	0.98	0.293
GM3	33.49	2.04	13.22	0.93	0.280
GM3	34.49	2.04	13.26	0.89	0.267
NL3	30.40	2.81	14.44	1.28	0.258
NL3	31.41	2.81	14.48	1.20	0.249
NL3	32.40	2.80	14.51	1.11	0.241
NL3	33.40	2.80	14.54	1.04	0.232
NL3	34.40	2.79	14.61	0.98	0.225
NL $\rho$	30.49	2.11	12.93	1.12	0.340
NL $\rho$	31.49	2.11	12.97	1.05	0.323
NL $\rho$	32.49	2.11	13.01	1.00	0.308
NL $\rho$	33.49	2.11	13.07	0.95	0.295
NL $\rho$	34.49	2.10	13.13	0.90	0.279

TABLE VI. Neutron star main properties without  $\delta$  meson.

### B. Fixing the slope $L$

In a second attempt, with the inclusion of the  $\delta$  meson, we fix the slope and vary the symmetry energy to study the influence of this quantity independently. The parameters utilized in this approach are presented in Tables VII, VIII, IX and X for GM1, GM3, NL3 and NL $\rho$  respectively.

We plot the density dependent symmetry energy  $S$  and the the slope  $L(n)$  with fixed  $L$  for GM3 and NL $\rho$  parametrization in Fig. 5.

When we fix the slope, the  $S$  and  $L(n)$  curves always cross each other. The parametrizations that predict lower values of  $S$  and  $L(n)$  at low density always predict high values at higher densities, contrary to what was found in the previous section. This is a global effect, present in our four models. The reason is that alongside the repulsive

$(g_{\rho}/m_{\rho})^2 (fm^{-2})$	$(g_{\delta}/m_{\delta})^2 (fm^{-2})$	$S_0$ (MeV)	L (MeV)
9.577	1.68	30.16	99.9
8.435	1.26	31.28	99.9
7.282	0.84	32.38	99.9
6.120	0.42	33.46	99.9
4.936	0.00	34.49	99.9

TABLE VII.  $S_0$  values with GM1 for a fixed slope at 99.9 MeV

$(g_{\rho}/m_{\rho})^2 (fm^{-2})$	$(g_{\delta}/m_{\delta})^2 (fm^{-2})$	$S_0$ (MeV)	L (MeV)
12.521	2.40	30.15	95.7
10.850	1.80	31.32	95.7
9.025	1.20	32.42	95.7
7.183	0.60	33.48	95.7
5.319	0.00	34.49	95.7

TABLE VIII.  $S_0$  values with GM3 for a fixed slope at 95.7 MeV

$(g_{\rho}/m_{\rho})^2 (fm^{-2})$	$(g_{\delta}/m_{\delta})^2 (fm^{-2})$	$S_0$ (MeV)	L (MeV)
6.80	1.04	30.11	109.4
6.246	0.78	31.19	109.4
5.690	0.52	32.28	109.4
5.127	0.26	33.36	109.4
4.552	0.00	34.40	109.4

TABLE IX.  $S_0$  values with NL3 for a fixed slope at 109.4 MeV

$(g_{\rho}/m_{\rho})^2 (fm^{-2})$	$(g_{\delta}/m_{\delta})^2 (fm^{-2})$	$S_0$ (MeV)	L (MeV)
10.696	2.00	30.04	97.0
9.260	1.50	31.22	97.0
7.803	1.00	32.35	97.0
6.333	0.50	33.45	97.0
4.842	0.00	34.49	97.0

TABLE X.  $S_0$  values with NL $\rho$  for a fixed slope at 97.0 MeV

$\rho$  meson, the attractive  $\delta$  meson contributes both to the symmetry energy and the slope. The  $\delta$  meson, being scalar, dominates at low densities, while the  $\rho$  meson, being a vector meson, dominates at high densities. So, to fix the slope at certain value, the lower the  $S$  and the  $L(n)$  are at low densities, the higher they are at high density.

Now we study this crossing effect in neutron star properties. We plot the mass/radius relation in Fig. 6. When we fix the slope  $L$ , a curious behaviour appears. The radii of canonical  $1.4M_{\odot}$  in general decreases with the symmetry energy. This effect, as far as we know, has not been noticed before. Usually, when  $\delta$  meson is not included, the  $S_0$  is determined just by the  $\rho$  meson coupling, and its slope is uniquely obtained. A correlation between  $L$  and the neutron star radius is then seen [6]. When we fix the slope, with the help of the  $\delta$  meson, different values of  $S_0$  are then obtained, and the correlation is lost. So, al-

though the slope  $L$  give us significant information on the behaviour of the masses, it is not enough to determine the neutron star radius, since different parametrizations with the same value of  $L$  cause variations of up to 1.7 km.

We can also see, that for GM3 and  $NL\rho$ , as  $S_0$  increases the radius first increases a little, then strongly decreases. This behaviour could indicate that, in these parametrizations, the value utilized for the slope  $L$  (95.7 for GM3 and 97.0 for  $NL\rho$ ) is too large for a symmetry energy  $S_0$  around 30 MeV.

The maximum mass changes a little more than in the case without  $\delta$  meson, but it is still not significantly altered, being not superior to  $0.05M_\odot$ .

To study the DU process, we plot the proton fraction in Fig. 7. We see that the same behaviour present in the symmetry energy  $S$  and in the slope  $L(n)$  is observed in the proton fraction  $Y_p$ , i.e. the parametrizations with lower values of  $Y_p$  at low densities are those with higher values of it at high densities. The reason again lies in the competition between the scalar  $\delta$  meson and the vector  $\rho$  meson. The  $\delta$  meson dominates at low densities, reducing the mass of the neutrons and increasing the mass of the protons, favouring neutron population. However, at high densities the  $\rho$  meson dominates, reducing the proton chemical potential. This inversion of lower/higher proton fraction in all models happens for densities above the critical value of  $x_{DU}$ .

The corresponding neutron star mass that allows the DU process is shown in Fig. 8. We see that, in general, increasing the symmetry energy  $S_0$  leads to a reduction of the minimum mass that enables the DU process, as in the case without  $\delta$  meson. It implies that, if on one hand the symmetry energy  $S_0$  has little influence on the radius of the canonical  $1.4M_\odot$  neutron star, on the other hand, it has a strong influence on the minimum mass that enables DU process, (although the slope  $L$  still contributes). We see that even different parametrizations result in very similar masses with similar values of  $S_0$ . Also, it is worth noting that when the symmetry energy increases from  $\approx 30$  to  $\approx 31$  MeV, the minimum masses for GM3 and  $NL\rho$  also increase. This effect is similar to the one present in the radius/symmetry energy relation, and again could indicate that the values of  $L$  are too large for  $S_0$  around 30 MeV.

We resume this section in Table XI.

We see that although different values of the symmetry energy produce different minimum masses that enable the DU process, the central density  $n$  are very similar. This is due to the fact that the proton fractions cross each other in a density close to the  $x_{DU}$ .

### C. Fixing the symmetry energy $S_0$

Finally, our last approach is to fix the  $S_0$  value to study the direct influence of the slope  $L$ . The parameters obtained with this approach are presented in Tables XII,

Model	$S_0$ (MeV)	$M_{max}/M_\odot$	$R_{1.4M_\odot}$	$M_{DU}/M_\odot$	$n_{DU}$ ( $fm^{-3}$ )
GM1	30.16	2.44	15.56	1.41	0.266
GM1	31.28	2.42	15.29	1.33	0.265
GM1	32.38	2.41	14.98	1.24	0.262
GM1	33.46	2.39	14.50	1.10	0.258
GM1	34.49	2.38	13.91	0.98	0.255
GM3	30.15	2.09	14.29	1.15	0.277
GM3	31.32	2.09	14.70	1.18	0.275
GM3	32.42	2.09	14.63	1.16	0.274
GM3	33.48	2.07	14.17	1.05	0.271
GM3	34.49	2.04	13.26	0.89	0.267
NL3	30.11	2.83	15.57	1.35	0.237
NL3	31.19	2.82	15.40	1.27	0.235
NL3	32.28	2.81	14.20	1.17	0.231
NL3	33.36	2.80	14.93	1.07	0.228
NL3	34.40	2.79	14.61	0.98	0.225
$NL\rho$	30.04	2.16	14.44	1.22	0.290
$NL\rho$	31.22	2.16	14.55	1.23	0.289
$NL\rho$	32.35	2.14	14.33	1.16	0.287
$NL\rho$	33.45	2.12	13.88	1.05	0.284
$NL\rho$	34.49	2.10	13.13	0.90	0.279

TABLE XI. Neutron star main properties with fixed  $L$ .

XIII, XIV and XV for the GM1, GM3, NL3 and  $NL\rho$  respectively. Note that GM1 and GM3 parametrizations keep the original value of  $S_0$ , fixed at 32.49 MeV. However, for  $NL\rho$  and NL3, we change the values from 30.49 MeV to 31.49 MeV and from 37.40 MeV to 33.40 MeV respectively, so that the the  $L$  values are no more than 1 MeV apart from each other.

$(g_\rho/m_\rho)^2$ ( $fm^{-2}$ )	$(g_\delta/m_\delta)^2$ ( $fm^{-2}$ )	$S_0$ (MeV)	$L$ (MeV)
14.687	3.00	32.49	118.4
12.991	2.50	32.49	113.9
11.287	2.00	32.49	109.6
9.578	1.50	32.49	105.4
7.858	1.00	32.49	98.5
4.410	0.00	32.49	93.9

TABLE XII.  $L$  values with GM1 for a fixed symmetry energy at 32.49 MeV

$(g_\rho/m_\rho)^2$ ( $fm^{-2}$ )	$(g_\delta/m_\delta)^2$ ( $fm^{-2}$ )	$S_0$ (MeV)	$L$ (MeV)
13.620	2.50	32.49	103.3
11.864	2.00	32.49	100.4
10.103	1.50	32.49	97.5
8.336	1.00	32.49	94.8
4.791	0.00	32.49	89.7

TABLE XIII.  $L$  values with GM3 for a fixed symmetry energy at 32.49 MeV

If the symmetry energy is fixed, the  $\delta$  meson always forces the slope to increase, as pointed in Ref. [8]. We also see that, although we are able to always construct

$(g_\rho/m_\rho)^2 (fm^{-2})$	$(g_\delta/m_\delta)^2 (fm^{-2})$	$S_0$ (MeV)	$L$ (MeV)
12.444	2.50	33.40	139.2
10.828	2.00	33.40	132.1
9.204	1.50	33.40	125.3
7.571	1.00	33.40	118.8
4.280	0.00	33.40	106.9

TABLE XIV.  $L$  values with NL3 for a fixed symmetry energy at 33.40 MeV

$(g_\rho/m_\rho)^2 (fm^{-2})$	$(g_\delta/m_\delta)^2 (fm^{-2})$	$S_0$ (MeV)	$L$ (MeV)
12.795	2.50	31.49	105.1
11.064	2.00	31.49	101.4
9.331	1.50	31.49	97.9
7.589	1.00	31.49	94.5
4.070	0.00	31.49	88.0

TABLE XV.  $L$  values with NL $\rho$  for a fixed symmetry energy at 31.49 MeV

an EoS with reasonable values of symmetry energy, some parametrizations have too large values of  $L$  ( $L > 113$  MeV). We keep these parametrizations for the sake of comparison.

We plot the density dependent symmetry energy  $S$  and the slope  $L(n)$  for this approach in Fig. 9 for GM1 and NL $\rho$  parametrization. Fixing  $S_0$  rather than fixing  $L$  causes the crossing of the curves to take place at lower densities. When we fix the slope  $L$ , the crossing of  $L(n)$ , which obviously always happened at  $n = n_0$  in the previous case, now happens at densities around  $0.6n_0$ , while the symmetry energy crossing, which happened around  $1.8n_0$ , now obviously happens at  $n = n_0$ .

We plot the TOV solution in Fig. 13. The effect of the slope  $L$  on neutron star properties was already studied in previous works [6, 11, 12]. Increasing the slope, the radii of canonical  $1.4M_\odot$  increases, as pointed out in ref. [6]. However, we can see that there is a limit. If the slope increases too much, the radii begins to drop again. We found that there is a maximum value of the neutron star radius. This maximum possible value could also indicate that there is a theoretical superior limit of acceptable values for the slope  $L$  for a fixed symmetry energy  $S_0$ . Moreover, as pointed out earlier, the fact that a fixed  $L$  produces differences of up to 1.7 km on the radii of the canonical  $1.4M_\odot$  indicates that although the slope gives us insight about the radii it is not enough to fully determine it. And again, the symmetry energy and its slope have almost no influence on the maximum mass of the neutron star.

Now we return to the DU process and plot the proton fraction in Fig. 11. Fixing the symmetry energy  $S_0$  causes the crossing to happens for densities below those which enable DU process. This is expected since this behaviour was already found in the density dependent symmetry energy  $S_0$ , and its slope  $L(n)$ .

The minimum mass that enables DU process for fixed

symmetry energy is plotted in Fig. 12 from where we see that there is an oscillation in the mass, that could again be associated with a too large value of  $L$ . It is interesting to note that although the NL3 has a higher value of maximum mass, GM1 produces a larger minimum mass which enables DU process.

The main results are shown in Table XVI.

Model	$L$ (MeV)	$M_{max}/M_\odot$	$R_{1.4M_\odot}$	$M_{DU}/M_\odot$	$n_{DU} (fm^{-3})$
GM1	93.9	2.39	13.80	1.10	0.279
GM1	98.5	2.43	15.17	1.30	0.267
GM1	105.4	2.44	15.58	1.28	0.250
GM1	109.6	2.44	15.81	1.31	0.243
GM1	113.9	2.44	15.85	1.30	0.237
GM1	118.4	2.40	14.29	1.02	0.232
GM3	89.7	2.04	13.16	0.98	0.293
GM3	94.8	2.09	14.48	1.15	0.275
GM3	97.5	2.10	14.68	1.15	0.267
GM3	100.4	2.09	14.58	1.11	0.260
GM3	103.3	2.07	14.23	1.03	0.254
NL3	106.9	2.80	14.54	1.04	0.232
NL3	118.8	2.83	15.65	1.17	0.219
NL3	125.3	2.83	15.86	1.19	0.213
NL3	132.1	2.83	15.84	1.18	0.209
NL3	139.2	2.82	15.56	1.16	0.206
NL $\rho$	88.0	2.11	12.97	1.05	0.323
NL $\rho$	94.5	2.16	14.24	1.19	0.298
NL $\rho$	97.9	2.17	14.49	1.20	0.285
NL $\rho$	101.4	2.16	14.43	1.16	0.276
NL $\rho$	105.1	2.15	14.10	1.09	0.269

TABLE XVI. Neutron star main properties with fixed  $S_0$ .

Finally we return to the question of the radii of the canonical  $1.4M_\odot$ . We pointed out that the slope alone does not give us enough information to determine them with precision. We rise a hypothesis that it is not the slope  $L$  but the variation of  $L(n)$  at sub-threshold densities that is correlated with the neutron star radii.

We have arbitrarily calculated the value  $\Delta L = L(1.25) - L(0.75)$  and plotted the results of all three approaches in Fig. 13.

We see that the neutron stars radii grow with  $\Delta L$ , reach a maximum, and drop again. This explains the fact that the same slope causes variations of up to 1.7 km in the radii and the oscillation in the radii with the increase of the slope. We can also see that there is a maximum value of the radii that depends on  $\Delta L$ .

Moreover, this could indicate that the values of  $\Delta L$  beyond the maximum radius are too large, limiting the maximum value for the slope  $L$ . For GM1 and NL3 these values are 113.9 MeV and 125.3 MeV for  $S_0$  equal to 32.49 MeV and 33.40 MeV respectively. The NL3 value is ruled out, since experiments point to a maximum value of 113 MeV [16, 21] and not larger than 115 MeV [13] and the GM1 value is too close to the accepted limit. However, for GM3 and NL $\rho$  the values of  $L$  beyond the maximum radii are 97.5 MeV and 97.9 MeV for  $S_0$  equal to 32.49

MeV and 31.49 MeV respectively. The results can be even lower. For  $S_0$  equal to 30.15 MeV and 30.04 MeV in GM3 and NL $\rho$  respectively, the values of  $L$ , which respectively are 95.7 MeV and 97.0 MeV, yielding values of  $\Delta L$  that are already beyond the maximum radii, indicating a relatively low theoretical superior limit for the slope  $L$ .

#### IV. FINAL REMARKS AND CONCLUSIONS

In this work we discuss the role of the symmetry energy and the slope on neutron star properties. To accomplish that, we divide our study in three different fronts, varying both  $S_0$  and the related  $L$  in the traditional  $\sigma\omega\rho$  model, fixing  $L$  and varying  $S_0$  within the  $\sigma\omega\rho\delta$  model, and vice-versa. We then obtain the maximum masses of neutron star, the radii of the canonical  $1.4 M_\odot$ , and the minimum mass that enables direct URCA process for each case.

We see that the maximum mass is not very much influenced by both  $S_0$  and  $L$  and the differences are never larger than  $0.06M_\odot$ . Since the EoS of  $\beta$  stable matter is very little sensitive to the variations of the symmetry energy and its slope [6, 11], we do not plot these graphs, which can be easily found in the literature [3, 11, 12, 35, 36].

We have confirmed that the radii of the canonical  $1.4 M_\odot$  is not affected by the symmetry energy  $S_0$ , whereas in some cases the radii increase with it, while in others, there is a decrease. Nevertheless, the radii is correlated with a variation of the slope  $\Delta L$ . The radii increase with  $\Delta L$  up to a maximum value, then drop again. This behaviour can be associated with a maximum theoretical value of  $L$ , and provide a possible constraint to nuclear matter. Our models predict radii from 12.9 km to 15.9 km. We are unable to explain the large pulsars as RX J1856.5-3754 [37] with radius of 17 km, neither the very small ones as those pointed out in Ref. [20, 38] with radii lying between 9-12 km. Neutron stars with small radii, are generally related to very low slope  $L$ , as suggested in some works [19, 20]. There is a QHD model that reproduces a low slope, the FSU [39]. However, previous studies [6, 40] indicate that the maximum mass within the FSU model is only  $1.7 M_\odot$ , and in the light of the recent super massive pulsars [41, 42], the FSU model cannot represent the ultimate EoS of nuclear matter. These controversial results alongside the possibility of a slope as high as 170 MeV [22] led us to believe that the neutron star radii is still an open puzzle.

Finally we study the influence of the symmetry energy and its slope on direct URCA process, which is directly related to the proton fraction  $Y_p$ . The minimum mass that enables DU process changes dramatically with the symmetry energy  $S_0$ . Indeed the variation of the minimum mass can reach more than 50%. Studies of neutron star cooling [32, 33] should be used to constrain nuclear matter.

We next discuss the validity of our models in the light

of experimental constraints of nuclear matter besides the symmetry energy and the slope, based in the discussion presented in Ref. [13]. The first physical quantity checked in [13] is the compressibility  $K$ , where the experimental results point to values between 190 - 270 MeV. This implies that while GM3 and NL $\rho$  fulfil this constraint, GM1 and NL3 have to be used with care, since both have values of  $K$  higher than 270 as pointed out in Table I. Recently, new constraints from re-analysis of data on GMR energies [43, 44] became available, suggesting that the compressibility values could move to somewhat higher values, 250 - 315 MeV. If this is confirmed, then GM3 and NL $\rho$  are the parametrizations that would be slightly out of the desired range.

The second physical quantity is the pressure of symmetric matter up to densities five times the nuclear saturation density, based on Ref. [45]. This constraint was already studied in other works [6, 13, 46], and again, while it is satisfied by the GM3 and NL $\rho$ , GM1 and NL3 are outside the experimental region of the pressure. However, as pointed in Ref. [46], GM1 can fulfil this constraint if we assume that hyperons populates the nuclear matter at high density.

In Ref. [13], the  $S_0$  and  $L$  values are also discussed.  $S_0$  is assumed to lie between 30 - 35 MeV, exactly as indicated in ref. [16-18]; and the maximum value of  $L$  being 115 MeV, which is very close of 113 MeV [16, 21] used in our work.

Nuclear astrophysics also provide constraints for nuclear matter. For instance, the discovery of two super-massive pulsars [41, 42] indicates a moderate stiff EoS for high density. Moreover, the possible existence of a 2.7 solar mass, correspondent to the pulsar PSR J1311-3430 [47], indicates a very stiff EoS.

Since the  $\delta$  scalar-isovector meson always increase the slope [8], in this work we have studied models with high values of  $L$ . The next step of our work is study models with low slope adding a non linear  $\omega - \rho$  coupling as in the FSU parametrization [39]. Although the FSU model seems to fail the description of super massive pulsars, we can add this term in the standard parametrizations, as we did with the  $\delta$  meson, and check if there is analogous results as a minimum neutron star radii.

Moreover, at high densities, strange content particles can be created [3]. However, they bring several ambiguities since we do not know the strength of the hyperon-meson interaction [46, 48] implying that the maximum mass can vary up to 100% [3]. Also, when hyperons are present, strange mesons could be important to mediate the hyperon-hyperon interactions [46, 48-50]. Alongside hyperons, strong magnetic fields [51], strongly affects the macroscopic properties of the neutron star. Works along these lines are in progress.

#### Acknowledgments

This work was partially supported by CNPq (Brazil), CAPES (Brazil) and FAPESC (Brazil) under project



- 
- [1] B. D. Serot, Rep. Prog. Phys. **55**, 1855 (1992)
- [2] N. K. Glendenning, Astrophys. J. **293**, 470 (1985)
- [3] N. K. Glendenning, *Compact Stars - Nuclear physics, Particle physics, and General relativity*, Springer, New York - Second Edition (2000)
- [4] A. Schmitt, *Dense Matter in Compact Stars*, Springer, Berlin (2010)
- [5] M. Camenzind, *Compact Objects in Astrophysics: White Dwarfs, Neutron Stars and Black Holes* Springer, Berlin (2007)
- [6] R. Cavagnoli, D. P. Menezes, C. Providencia, Phys. Rev. C **84**, 065810 (2011)
- [7] S. Kubis, M. Kutschera, Phys. Lett. B **399**, 191 (1997)
- [8] B. Liu et al, Phys. Rev. C **65**, 045201 (2002)
- [9] R. J. Furnstahl, Nucl. Phys. A **706**, 85 (2002)
- [10] V. Greco et al, Phys. Rev. C **67**, 015203 (2003)
- [11] D. P. Menezes, C. Providencia Phys. Rev. C **70**, 058801 (2004)
- [12] B. Liu et al, Eur. Phys. J. A **25**, 293 (2005)
- [13] M. Dutra et al, arXiv:1405.3633
- [14] N. K. Glendenning, S. A. Moszkowski, Phys. Rev. Lett. **67**, 2414 (1991)
- [15] G. A. Lalazissis, J. Konig, P. Ring, Phys. Rev. C **55**, 540 (1997)
- [16] M. B. Tsang et al, Phys. Rev. C **86**, 015803 (2012)
- [17] Z. Y. Sun et al, Phys. Rev. C **82**, 051603(R) (2010)
- [18] A. Carbone et al, Phys. Rev. C **81**, 041301 (2010)
- [19] J. M. Lattimer, Y. Lim, Astrophys. J. **771**, 51 (2013)
- [20] A. W. Steiner, S. Gandolfi, Phys. Rev. Lett. **108**, 081102 (2012)
- [21] Lie-Wen Chen, Che Ming Ko, and Bao-An Li, Phys. Rev. C **72**, 064309 (2005)
- [22] M. D. Cozma et al, Phys. Rev. C **88**, 044912 (2013)
- [23] J. Boguta and A.R. Bodmer, Nucl. Phys. A **292**, 413 (1977)
- [24] Kerson Huang: *Introduction to Statistical Physics*, Taylor & Francis, London - (2001)
- [25] J. R. Oppenheimer, G. M. Volkoff, Phys. Rev. **33**, 374 (1939)
- [26] G. Baym, C. Pethick, P. Sutherland, Astrophys. J. - **170**, 299 (1971)
- [27] R. Machleidt, Adv. Nucl. Phys. **19**, 189 (1989)
- [28] X. Roca-Maza et al, Phys. Rev. C, **84** 054309 (2011)
- [29] J. M. Lattimer et al, Phys. Rev. Lett. **66**, 2701 (1991)
- [30] T. Klahn et al, Phys. Rev. C **74**, 0035802 (2006)
- [31] S Tsuruta et al, Astrophys. J. Lett. **571**, L143 (2002)
- [32] C. J. Horowitz, J. Piekarewicz, Phys.Rev. C **66** 055803 (2002)
- [33] D. G. Yakovlev, C. J. Pethick, Ann. Rev. Astron. Astrophys. **42**, 169 (2004)
- [34] H. S. Than, D. T. Khoa, N. V. Giai, Phys. Rev. C **80**, 064312 (2009)
- [35] M. G. Paoli, D. P. Menezes, Eur. Phys. J. A **46**, 413 (2010)
- [36] L. L. Lopes, D. P. Menezes, Braz. J. Phys. **42**, 428 (2012)
- [37] Wynn C. G. Ho et al, Mon. Not. R. Astron. Soc. **375**, 821 (2007).
- [38] S. Guillot, M. Servillat, N.A. Webb and R.E. Rutledge, Astrophys. J. **772**, 7 (2013)
- [39] B .G. Todd-Rutel, J. Piekarewicz, Phys. Rev. Lett. **95**, 122501 (2005)
- [40] G. Shen, C. J. Horowitz, E. O'Connor, Phys. Rev. C **83**, 065808 (2011)
- [41] P. B. Demorest, et al. Nature, **467**, 1081 (2010)
- [42] J. Antoniadis et al, Science **340**, 1233232 (2013)
- [43] D. H. Youngblood et al., Phys. Rev. C **69**, 034315 (2004)
- [44] M. Uchida et al., Phys. Rev. C **69**, 051301 (2004); M. Uchida et al., Phys. Letts. B **557**, 12 (2003)
- [45] P. Danielewicz et al, Science **298**, 1592 (2002).
- [46] L. L. Lopes, D. P. Menezes, Phys. Rev. C **89**, 025805 (2014)
- [47] R. Romani et al, Astrophys. J. Lett **760**, L36 (2012)
- [48] S. Weissenborn, D. Chatterjee, J. Schaffner-Bielich, Phys. Rev. C **85**, 065802 (2012)
- [49] J. Ellis, J. I. Kapusta, K. A. Olive, Nucl. Phys.B **348**, 345 (1991)
- [50] R. Cavagnoli, D. P. Menezes, Braz. J. Phys. **35**, 869 (2005)
- [51] Q. Peng, H. Tong, Mon. Not. R. Astron. Soc. **378**, 159 (2007).

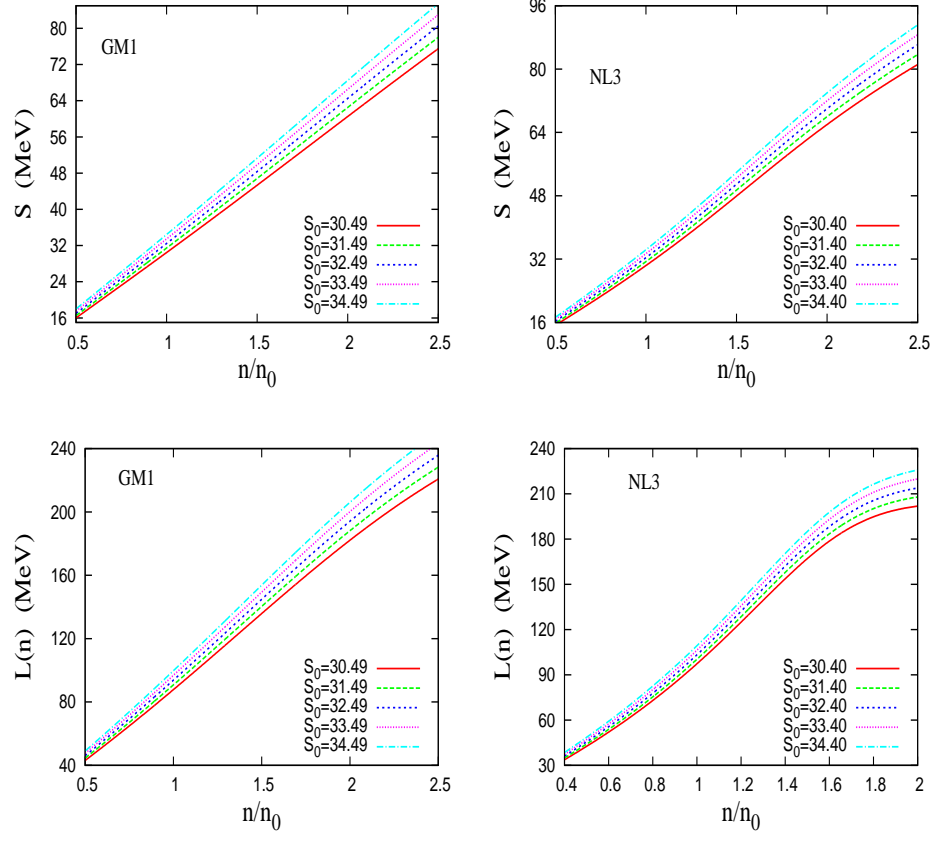


FIG. 1. (Color online) (Top) Symmetry energy  $S$  as function of density and (Bottom) slope of the symmetry energy  $L(n)$  as function of density with the  $\sigma\omega\rho$  model.

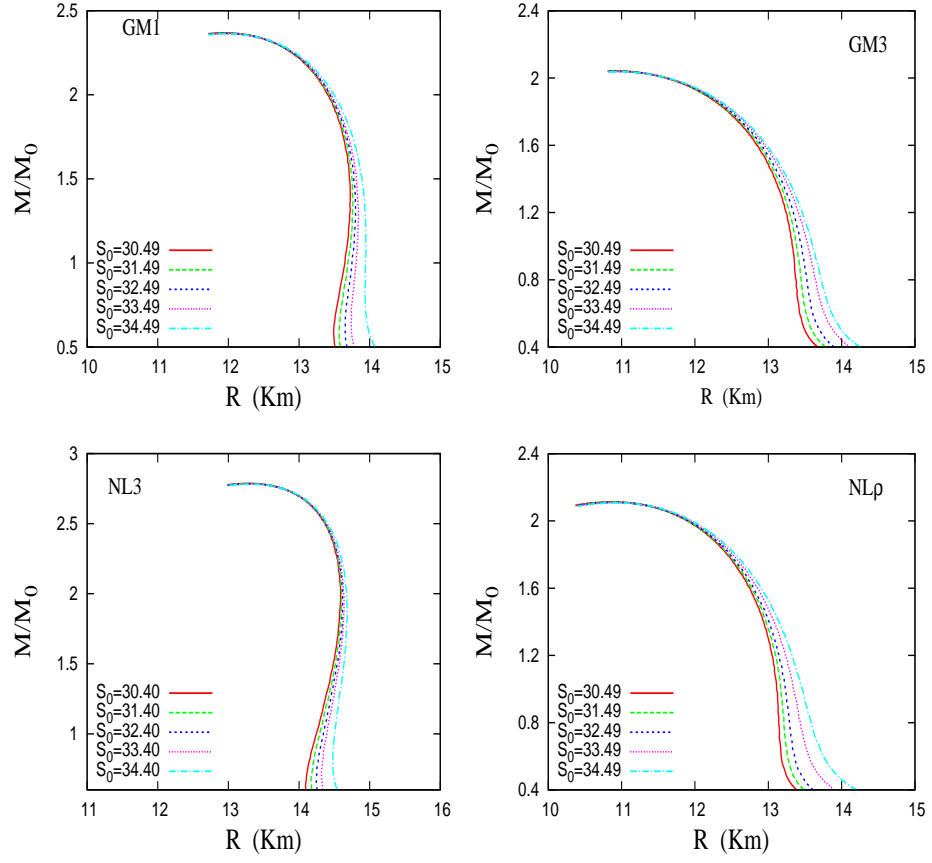


FIG. 2. (Color online) Neutron star mass-radius relation without  $\delta$  meson.

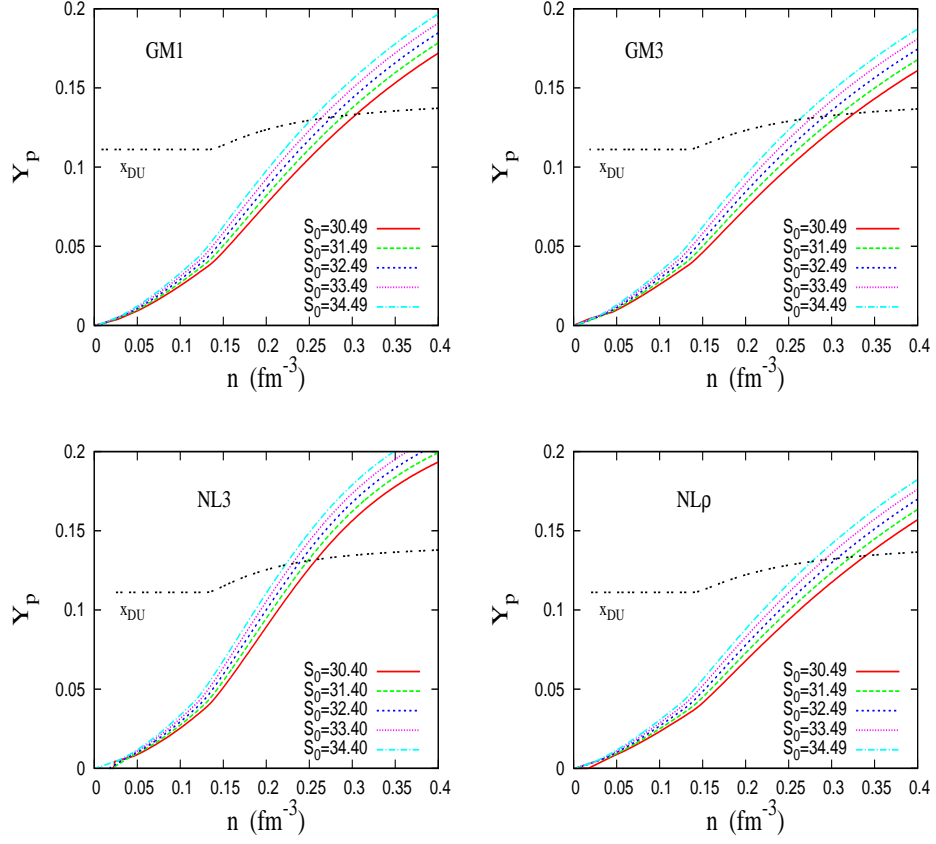


FIG. 3. (Color online) Proton fraction  $Y_p$  and the critical value  $x_{DU}$  without  $\delta$  meson.

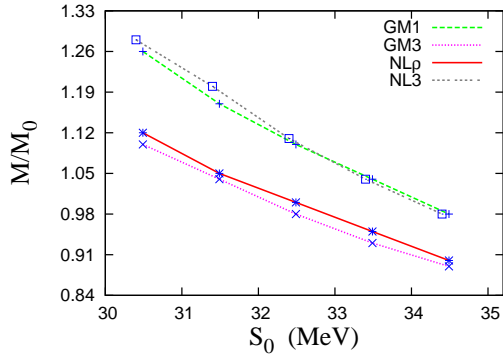


FIG. 4. (Color online) Minimum mass that enable DU process without  $\delta$  meson

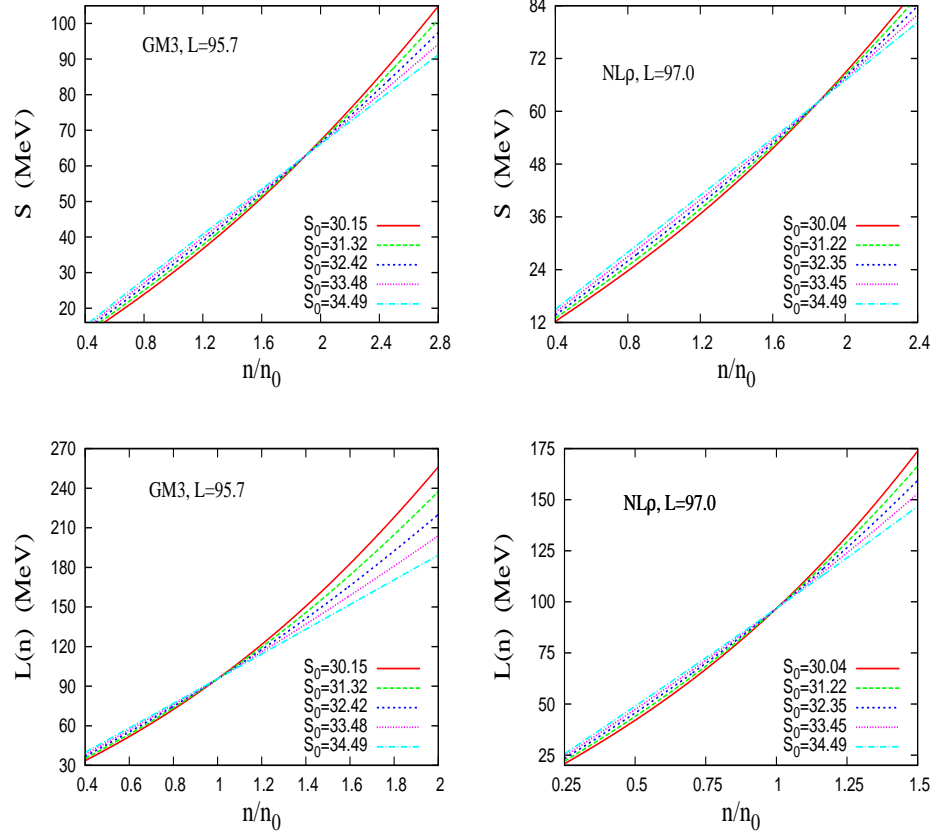


FIG. 5. (Color online) (Top) Symmetry energy  $S$  as function of density and (Bottom) slope of the symmetry energy  $L(n)$  as function of density with fixed  $L$ .

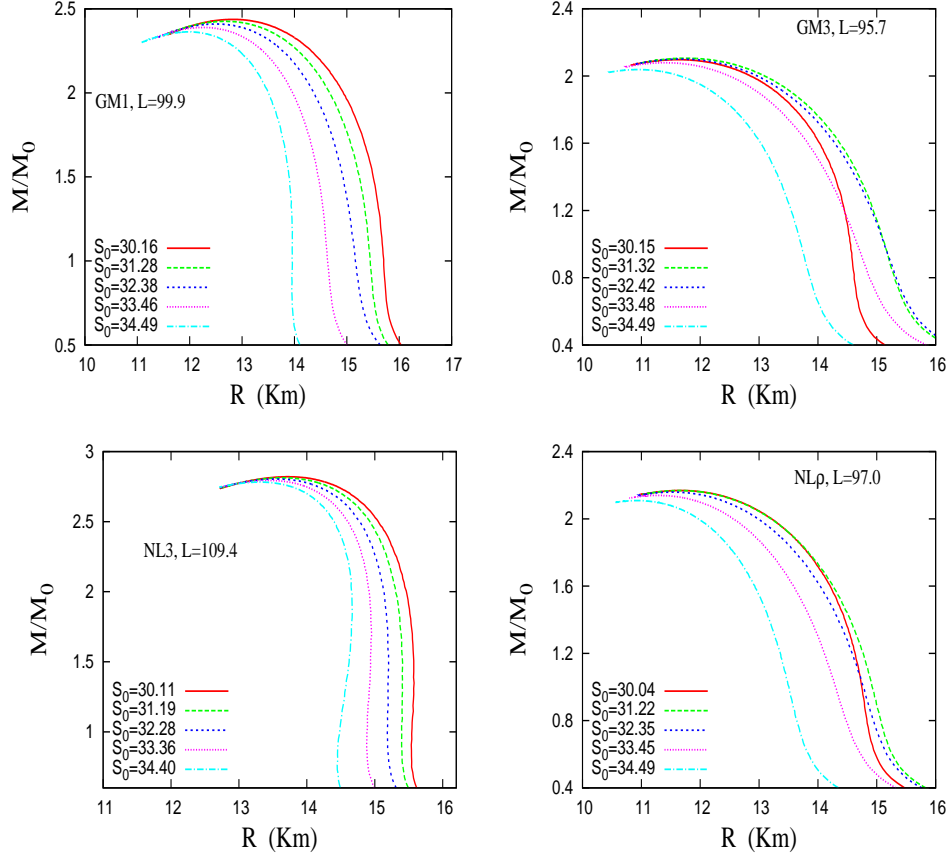


FIG. 6. (Color online) Neutron star mass-radius relation with fixed  $L$ .

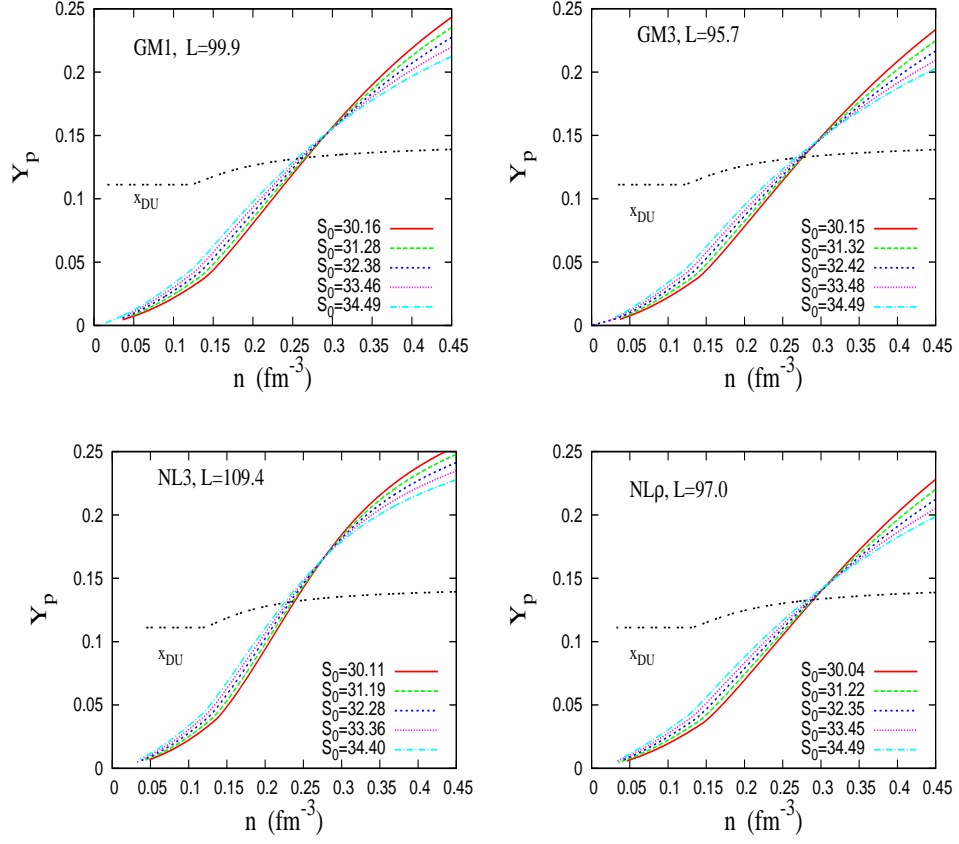


FIG. 7. (Color online) Proton fraction  $Y_p$  and the critical value  $x_{DU}$  with fixed  $L$ .

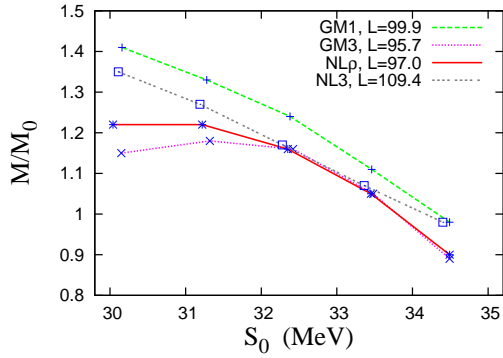


FIG. 8. (Color online) Minimum mass that enable DU process with fixed  $L$ .

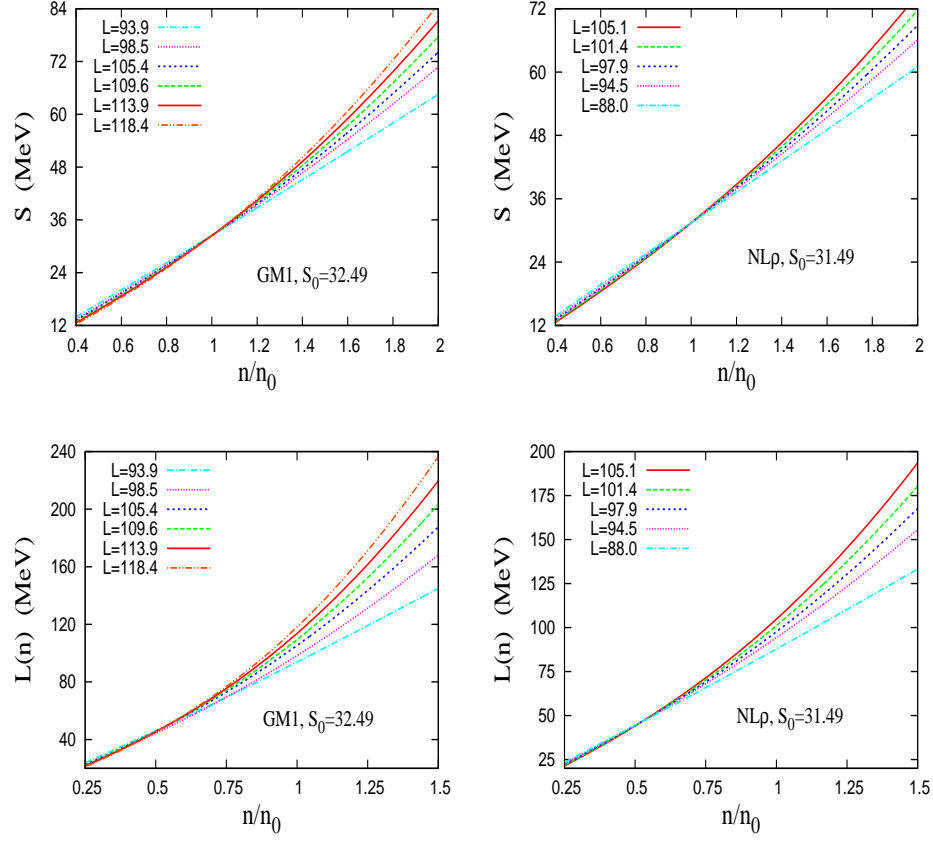


FIG. 9. (Color online) (Top) Symmetry energy  $S$  as function of density and (Bottom) slope of the symmetry energy  $L(n)$  as function of density with fixed  $S_0$ .



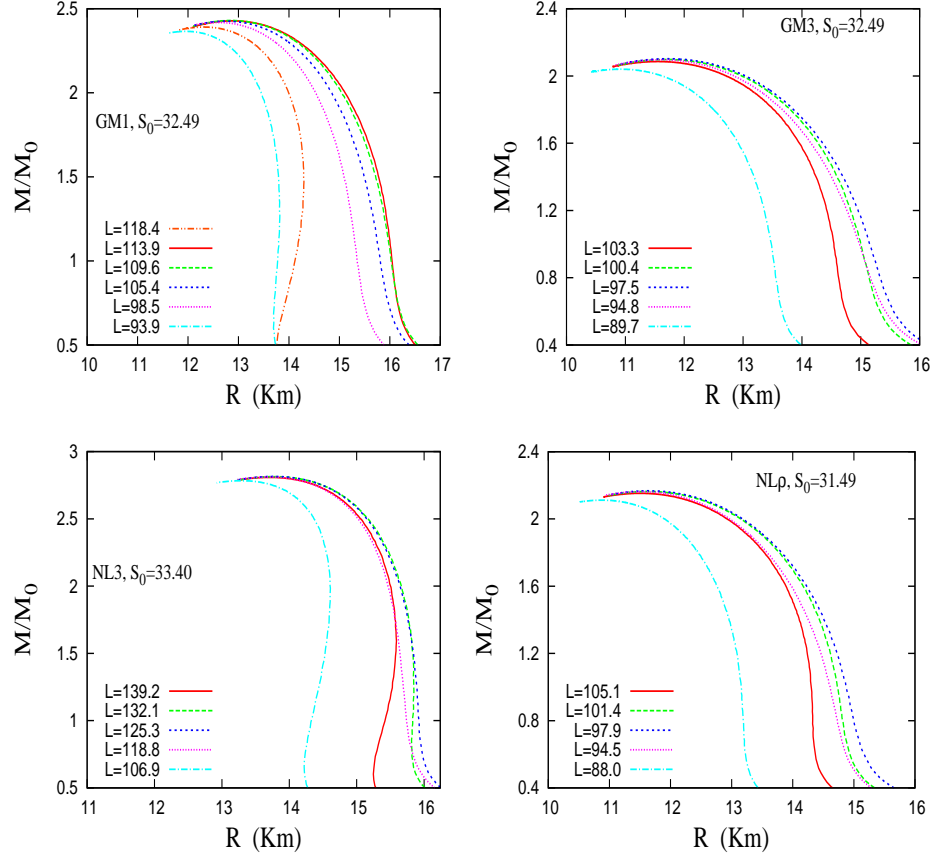


FIG. 10. (Color online) Neutron star mass-radius relation with fixed  $S_0$ .

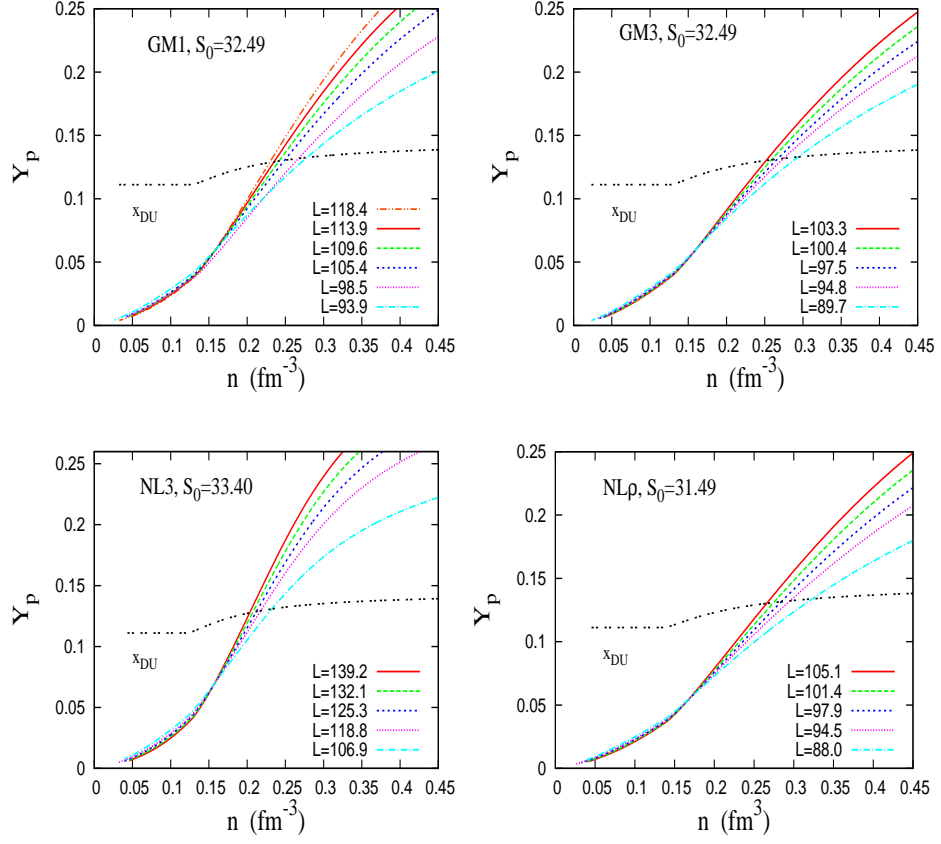


FIG. 11. (Color online) Proton fraction  $Y_p$  and the critical value  $x_{DU}$  with fixed  $S_0$ .

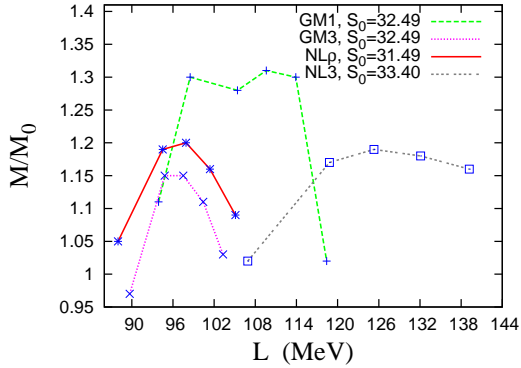


FIG. 12. (Color online) Minimum mass that enable DU process with fixed  $S_0$ .

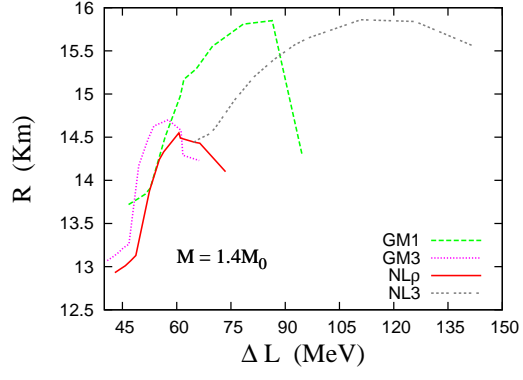


FIG. 13. (Color online) Neutron star radii as function of the variation of the slope  $\Delta L$ .